

Highly-Sensitive Gate/Body-Tied MOSFET-Type Photodetector Using Multi-Finger Structure

Juneyoung Jang¹, Pyung Choi¹, Hyeon-June Kim², and Jang-Kyoo Shin^{1,*}

Abstract

In this paper, we present a highly-sensitive gate/body-tied (GBT) metal-oxide semiconductor field-effect transistor (MOSFET)-type photodetector using multi-finger structure whose photocurrent increases in proportion to the number of fingers. The drain current that flows through a MOSFET using multi-finger structure is proportional to the number of fingers. This study intends to confirm that the photocurrent of a GBT MOSFET-type photodetector that uses the proposed multi-finger structure is larger than the photocurrent per unit area of the existing GBT MOSFET-type photodetectors. Analysis and measurement of a GBT MOSFET-type photodetector that utilizes a multi-finger structure confirmed that photocurrent increases in ratio to the number of fingers. In addition, the characteristics of the photocurrent in relation to the optical power were measured. In order to determine the influence of the incident the wavelength of light, the photocurrent was recorded as the incident the wavelength of light varied over a range of 405 to 980 nm. A highly-sensitive GBT MOSFET-type photodetector with multi-finger structure was designed and fabricated by using the Taiwan semiconductor manufacturing company (TSMC) complementary metal-oxide-semiconductor (CMOS) 0.18 um 1-poly 6-metal process and its characteristics have been measured.

Keywords: Multi-finger, Gate/body-tied, Photodetector, Photocurrent, Wavelength

1. INTRODUCTION

Digital still cameras and mobile phones that effectively acquire video information using image sensors are widely used. The manufacturing processes and application methods can be broadly classified into charge coupled device (CCD) type image sensors and complementary metal-oxide-semiconductor (CMOS) type image sensors. CMOS image sensors are both highly integrated and highly efficient tools for acquiring image information. CMOS image sensors allow for the use of peripheral circuits that convey a number of benefits pertaining to unit pixel size, image resolution, power consumption and cost. These advantages are utilized in various fields, and related research is currently being

conducted [1-3]. Indicators for evaluating CMOS image sensors include dynamic range, sensitivity, and resolution. Sensitivity is the amount of signal voltage relative to the amount of incident light. Higher sensitivity results in clearer images even in a dark environment as well as more signal power and consequently a larger signal-to-noise ratio. Recently, among the research fields involved with the study and production of image sensors, research on CMOS photodetectors has been of particular interest. The p-n junction photodetector commonly used in CMOS image sensors has a good dynamic range but has the disadvantage of low sensitivity. Types of photodetectors include p-n junction photodetectors, pinned photodiodes (PPDs), MOSFET photodetectors, and single photon avalanche photodiodes (SPADs) [4-10].

In this study, a GBT MOSFET-type photodetector using multi-finger structure has been designed and fabricated using the TSMC 0.18 um CMOS 1-poly 6-metal process. The drain current flowing through the MOSFET using multi-finger structure is proportional to the number of fingers [11-14]. It is attempted to confirm that the photocurrent of the GBT MOSFET-type photodetector using the presented multi-finger structure is larger than the photocurrent of the conventional GBT MOSFET-type photodetector per unit area.

The characteristics of the photocurrent according to the number

¹School of Electronic and Electrical Engineering,
Kyungpook National University
80 Daehak-ro, Buk-gu, Daegu, 41566, Korea

²School of Electrical Information Communication Engineering, Kangwon National University, 346 Jungang-ro, Samcheok-si, Gangwon-do 25913, Republic of Korea

*Corresponding author: jkshin@ee.knu.ac.kr

(Received: May 21, 2022, Revised: May 30, 2022, Accepted: May 31, 2022)

This is an Open Access article distributed under the terms of the Creative Commons Attribution Non-Commercial License(<https://creativecommons.org/licenses/by-nc/3.0/>) which permits unrestricted non-commercial use, distribution, and reproduction in any medium, provided the original work is properly cited.

of fingers and the characteristics of the photocurrent according to the intensity of the incident light were evaluated by measurement. In addition, the characteristics of the photodetector were comparatively analyzed in the wavelength range of 405 - 980 nm of the incident light.

2. EXPERIMENTAL

2.1 Multi-finger MOSFET

Fig. 1 (a) shows a layout of a conventional MOSFET and Fig. 1 (b) shows a layout of a MOSFET using multi-finger structure. The MOSFET has one gate, while the MOSFET using the multi-finger structure has five gates. The saturated drain current I_d of the MOSFET is as shown in the equation (1).

$$I_d = \mu_n C_{ox} W / 2L (V_{gs} - V_T)^2 \quad (1)$$

where V_{gs} is the voltage between the gate and source, C_{ox} is the gate capacity per unit area, and V_T is the threshold voltage. μ_n is the average electron mobility, and width (W) and length (L) are the effective channel width and length, respectively. The I_d of the multi-finger MOSFET is as shown in equation (2) [11-14].

$$I_d = \mu_n C_{ox} (W * N_f) / 2L (V_{gs} - V_T)^2 \quad (2)$$

where V_{gs} is the voltage between the gate and source, C_{ox} is the gate capacity per unit area, and V_T is the threshold voltage. μ_n is

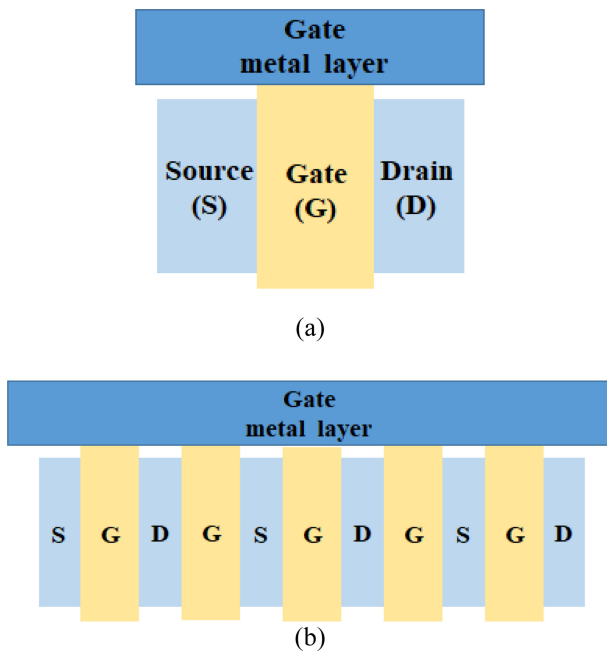


Fig. 1. (a) Layout of a conventional MOSFET and (b) layout of a MOSFET using multi-finger structure.

the average value of electron mobility, and W and L are the effective channel width and length, respectively. N_f is the number of fingers. It can be seen from the above equation that I_d increases as N_f increases.

2.2 GBT MOSFET-type photodetector using multi-finger structure

Fig. 2 (a) shows the symbol of a GBT p-channel MOSFET-type photodetector using multi-finger structure. In order to measure the photocurrent (I_{ph}) generated by the incident light on the active region of a GBT MOSFET-type photodetector using the multi-finger structure, a GBT MOSFET-type photodetector using the multi-finger structure was designed with the structure presented in Fig. 2 (a). Fig. 2 (b) shows that the gate node of the GBT p-channel MOSFET-type photodetector using the multi-finger structure is physically tied to the body node. In addition, it shows that each source node, drain node, and gate node are designed to be tied together. In the GBT MOSFET-type photodetector using the multi-finger structure, the area excluding the gate is shielded by a metal wire. Therefore, the light only enters the gate area.

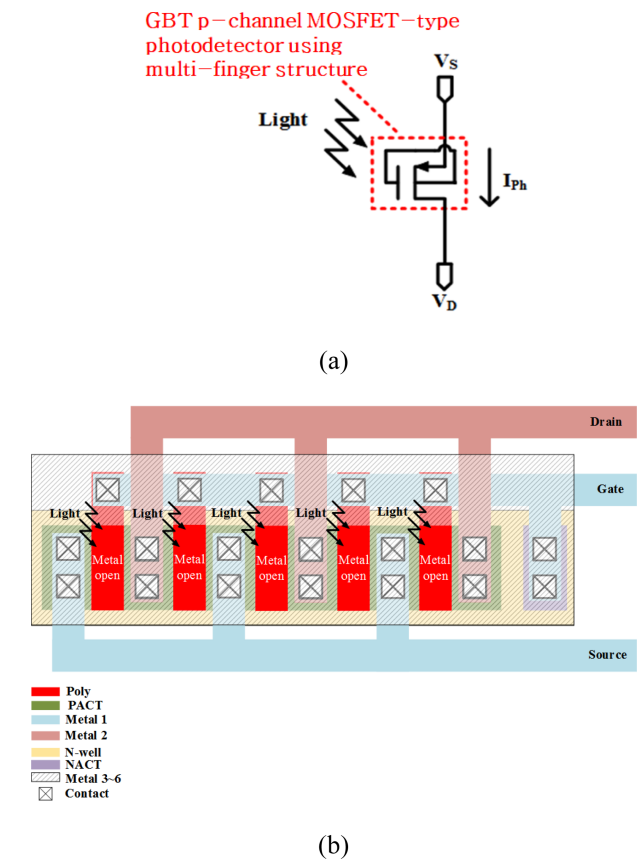


Fig. 2. GBT p-channel MOSFET-type photodetector using multi-finger structure; (a) symbol, (b) layout.

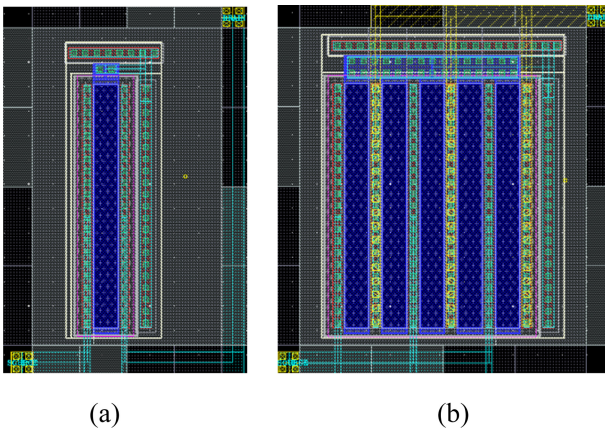


Fig. 3. Layout of the manufactured GBT MOSFET-type photodetector using multi-finger structure (a) $N_f = 1$ ($W/L = 10/1$) and (b) $N_f = 5$ ($W/L = 50/1$).

Some photons with short wavelengths are absorbed in the polysilicon gate, resulting in the reduction of sensitivity, while photons with long wavelengths are mostly absorbed by the substrate. Incident light passing through the gate creates electron-hole pairs in the depletion region. The holes drift towards the channels and the P substrate, and electrons accumulate in the N-wells due to the high potential barrier. Since the gate of the accumulated electrons is tied to the N-well, the gate voltage of the GBT MOSFET-type photodetector utilizing the multi-finger structure is reduced, and the potential barrier of the N-well is reduced. A channel is formed by a decrease in the gate voltage, and a current flows through the channel. In addition, the accumulated electrons generate an N-well negative voltage and generate positive feedback to the gate via the gate / N-well connection. The photocurrent of the GBT MOSFET-type photodetector is greatly amplified by this positive feedback mechanism [9-10]. A GBT MOSFET-type photodetector using the multi-finger structure has the same operating principle as the conventional GBT MOSFET-type photodetectors. However, since the photocurrent increases by the number of fingers, it has a higher photosensitivity for the same area.

Fig. 3 shows the layout of the manufactured GBT MOSFET-type photodetector using the multi-finger structure, which is designed for each of (a) $N_f = 1$ ($W/L = 10/1$) and (b) $N_f = 5$ ($W/L = 50/1$).

3. RESULTS AND DISCUSSIONS

Fig. 4 shows an experimental environment in which a probe

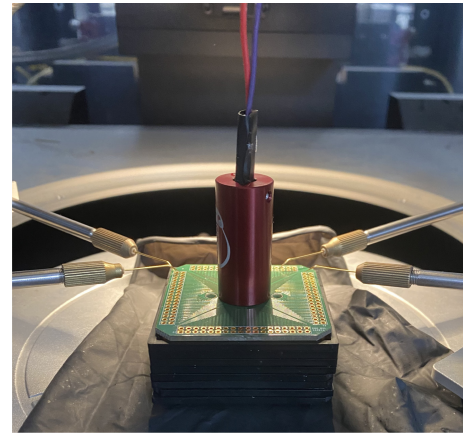


Fig. 4. Experimental environment for photocurrent measurement of photodetectors.

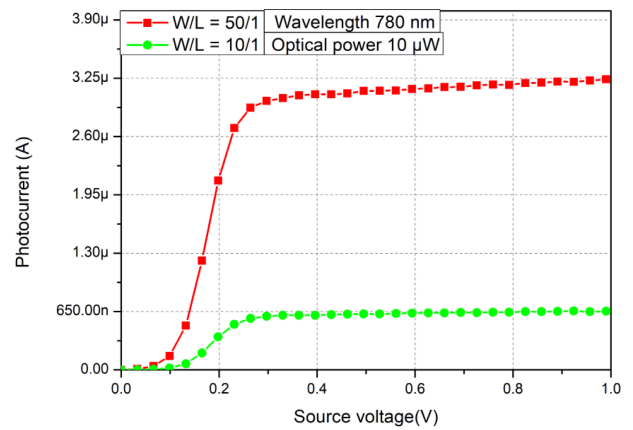


Fig. 5. Photocurrent measurement results according to the source voltage of the GBT MOSFET-type photodetector using the multi-finger structure $N_f = 1$ ($W/L = 10/1$) and $N_f = 5$ ($W/L = 50/1$).

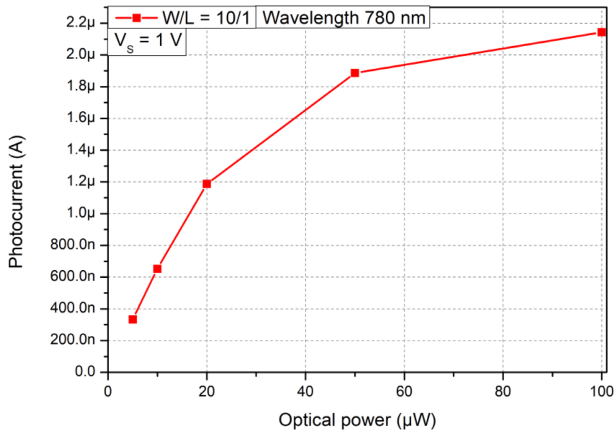
station was used to measure the photocurrent of the presented photodetector. Using laser diodes, the incident light was emitted at a total of 6 wavelengths of 405 nm, 520 nm, 650 nm, 780 nm, 850 nm, and 980 nm. A collimator was used to focus the light emitted by the laser diode onto the chip.

Fig. 5 shows the photocurrent measurement results relative to the source voltage of the GBT MOSFET-type photodetector using the multi-finger structure for the 780 nm wavelength. A laser diode with a wavelength of 780 nm was used as a light source, and the optical power was held constant at 10 μ W. Dark current of the photocurrent for the 780 nm wavelength was 60 pA, when $N_f = 5$ ($W/L = 50/1$) and $V_{SD} = 1$ V. This value is negligible compared to the photocurrent of the photodetector and thus neglected when calculating the photocurrent ratio.

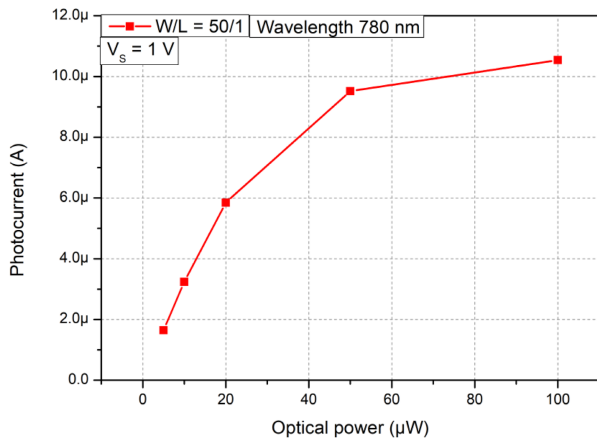
Table 1 shows the ratio of the measured photocurrent with respect to the number of fingers when $V_{SD} = 1$ V of the

Table 1. Ratio of the measured photocurrent by the number of fingers when $V_{SD} = 1$ V for the photodetectors in Fig. 5.

	W/L ($\mu\text{m}/\mu\text{m}$)	Photocurrent (A)	Photocurrent ratio
Conventional GBT ($N_f = 1$)	10/1	0.65μ	4.92
Multi-finger GBT ($N_f = 5$)	50/1	3.2μ	



(a)



(b)

Fig. 6. Photocurrent measurement results according to the optical power of the GBT MOSFET-type photodetector using multi-finger structure (wavelength 780 nm) (a) $N_f = 1$ ($W/L = 10/1$) and (b) $N_f = 5$ ($W/L = 50/1$).

photodetectors in Fig. 5. It can be seen that the ratio of the photocurrents is 4.92, meaning that the multi-finger GBT has a photocurrent approximately 5 times that of a conventional GBT when $N_f = 5$.

Fig. 6 shows the photocurrent measurement corresponding to the optical power of the GBT MOSFET-type photodetector using multi-finger structure. A laser diode with a wavelength of 780 nm

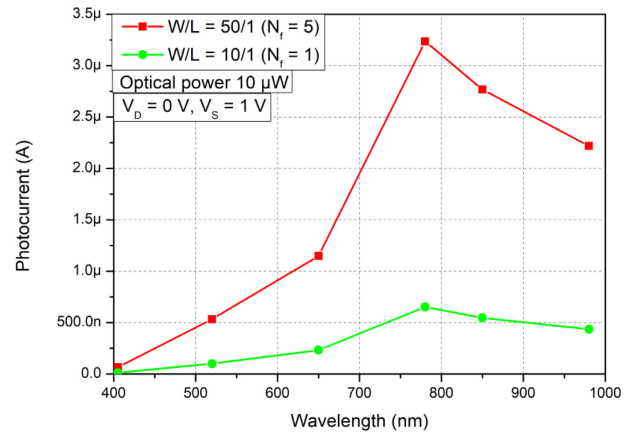


Fig. 7. Photocurrent measurement results according to wavelength of the GBT MOSFET-type photodetector using multi-finger structure for $N_f = 1$ ($W/L = 10/1$) and $N_f = 5$ ($W/L = 50/1$).

was used as the light source. The output optical power of the laser diode was measured under the conditions of 5, 10, 20, 50, and 100 μW . It can be seen that as the optical power increases, the photocurrent flowing through the photodetector increases, and as the intensity of the optical power increases, the rate of increase in the photocurrent decreases.

Fig. 7 shows the photocurrent measurement results for each wavelength of the GBT MOSFET-type photodetector using the multi-finger structure for $N_f = 1$ ($W/L = 10/1$) and $N_f = 5$ ($W/L = 50/1$). The wavelength of incident light of the laser diode used for the measurement was 405 nm - 980 nm. The optical power was equally set at 10 μW . In Fig. 7, when $N_f = 1$, the measured photocurrent at all wavelengths was in the range of about 1.29nA - 652nA. When $N_f = 5$, the photocurrent was in the range of about 6.67nA - 3.24 μA . As a result of measuring and comparing the photocurrents of the GBT MOSFET-type photodetector using the multi-finger structure, it was confirmed that the photocurrent increased about 5 times in proportion to the number of fingers at a wavelength of 405 nm - 980 nm. In addition, it was confirmed through measurement that the photocurrent of the GBT MOSFET-type photodetector using the multi-finger structure was maximized at an incident light wavelength of 780 nm. It can be seen that this result is similar to that of the conventional Si p-n junction photodetector [15-16]. Below 780 nm, as the wavelength decreases, more photons are absorbed near the surface, resulting in the decrease of photocurrent. Above 780 nm, as the wavelength increases, absorption coefficient decreases, resulting in the decrease of photocurrent.

4. CONCLUSIONS

In this paper, a highly-sensitive GBT MOSFET-type photodetector with multi-finger structure was designed and fabricated by using the TSMC CMOS 0.18 μm 1-poly 6-metal process. It was confirmed by measurement that the photocurrent of the GBT MOSFET-type photodetector using the multi-finger structure increased in proportion to the number of fingers. In addition, it was found that the photocurrent flowing through the photodetector increased as the optical power increased, and it was confirmed through measurements that the rate of increase in the photocurrent decreased as the intensity of the optical power increased. Then, when the wavelength of the incident light was measured in the range of 405 nm - 980 nm, it was confirmed through the measurement that it had a maximum photocurrent at the wavelength of 780 nm.

With the recent developments of processing technology, the area of the chip is gradually getting smaller, and the area of the photodetector is getting smaller as well. As the area of the photodetector becomes smaller, the photocurrent flowing through the photodetector also becomes smaller. However, with a GBT MOSFET-type photodetector using the multi-finger structure presented in this paper, it is possible to make a photodetector with high sensitivity while minimizing its area. Therefore, it is expected that the presented photodetector will be suitable for many applications requiring high sensitivity and small area in the visible and near infrared (NIR) ranges.

ACKNOWLEDGMENT

This research was supported by the Samsung Electronics Company and Basic Science Research Program through the National Research Foundation of Korea (NRF) funded by the Ministry of Education (2018R1D1A3B0704995213). We are grateful for these supports.

REFERENCES

- [1] L. Yao, K. Y. Yung, R. Khan, V. P. Chodavarapu, and F. V. Bright, "CMOS Imaging of Pin-Printed Xerogel-Based Luminescent Sensor Microarrays", *IEEE Sens. J.*, Vol. 10, No. 12, pp. 1824-1832, 2010.
- [2] E. R. Fossum, "CMOS image sensors: electronic camera-on-a-chip", *IEEE Trans. Electron Devices*, Vol. 44, No. 10, pp. 1689-1698, 1997.
- [3] M. Bigas, E. Cabruja, J. Forest, and J. Salvi, "Review of CMOS image sensors", *Microelectronics J.*, Vol. 37, No. 5, pp. 433-451, 2006.
- [4] H. Alaibakhsh and M. A. Karami, "Analytical Modeling of Pinning Process in Pinned Photodiodes", *IEEE Trans. Electron Devices*, Vol. 65, No. 10, pp. 4262-4368, 2018.
- [5] E. R. Fossum and D. B. Hondongwa, "A review of the pinned photodiode for CCD and CMOS image sensors", *IEEE J. Electron Devices Soc.*, Vol. 2, No. 3, pp. 33-43, 2014.
- [6] N. Tanaka, Y. Nakamura, and T. Ohmi, "A Novel Bipolar Imaging Device with Self-Noise-Reduction Capability", *IEEE Trans. Electron Devices*, Vol. 36, No. 1, pp. 31-38, 1989.
- [7] W. Shi and A. Pan, "Mixed Design of SPAD Array Based TOF for Depth Camera and Unmanned Vehicle Applications", *SMACD 2018 - 15th Int. Conf. Synth. Model. Anal. Simul. Methods Appl. to Circuit Des.*, pp. 277-280, 2018.
- [8] J. Kekkonen, T. Talala, J. Nissinen, and I. Nissinen, "On the Spectral Quality of Time-Resolved CMOS SPAD-Based Raman Spectroscopy with High Fluorescence Backgrounds", *IEEE Sens. J.*, Vol. 20, No. 9, pp. 4635-4645, 2020.
- [9] S. -H. Seo, K. -D. Kim, M. -W. Seo, J. -S. Kong, J. -K. Shin, and P. Choi, "Optical characteristics of an N-Well/gate-tied PMOSFET-type photodetector with built-in transfer gate for CMOS image sensor", *Sens. Mater.*, Vol. 19, No. 7, pp. 435-444, 2007.
- [10] H. Kwen, S. -H. Kim, J. Lee, P. Choi, and J. -K. Shin, "Simulation of High-Speed and Low-Power CMOS Binary Image Sensor Based on Gate/Body-Tied PMOSFET-Type Photodetector Using Double-Tail Comparator", *J. Sens. Sci. Technol.*, Vol. 29, No. 2, pp. 82-88, 2020.
- [11] F. Haddad, A. Ben Hammadi, and S. Saad, "Effect of Multi-Finger Gate MOSFET on RF Analog Integrated Circuit Performances", pp. 20-21, 2020.
- [12] C. Y. Lin, P. H. Chang, and R. K. Chang, "Impact of Inner Pickup on ESD Robustness of Multifinger MOSFET in 28-nm High-k/Metal Gate CMOS Process", *IEEE Trans. Device Mater. Reliab.*, Vol. 15, No. 4, pp. 633-636, 2015.
- [13] K. Hsuan Meng, Z. Chen, and E. Rosenbaum, "Compact distributed multi-finger MOSFET model for circuit-level ESD simulation," *Microelectron. Reliab.*, Vol. 63, pp. 11-21, 2016.
- [14] W. Effect, "A Study on Improved SPICE MOSFET RF Model Considering Wide Width Effect", No. 77, pp. 77-82, 2008.
- [15] J. Jang, P. Choi, H.-K. Lyu, and J.-K. Shin, "Photocurrent Characteristics of Gate/Body-Tied MOSFET-Type Photodetector with High Sensitivity", *J. Sens. Sci. Technol.*, Vol. 31, No. 1, pp. 1-5, 2022.
- [16] J. Jang, S. -H. Seo, J. Kong, and J. -K. Shin, "Effects of Transfer Gate on the Photocurrent Characteristics of Gate/Body-Tied MOSFET-Type Photodetector", *J. Sens. Sci. Technol.*, Vol. 31, No. 1, pp. 12-15, 2022.